

# Ocean current observations by infrared and visual Large Scale Particle Image Velocimetry (LSPIV)

Nick Ruessmeier<sup>1,2</sup>

<sup>1</sup> Jade University of Applied Sciences  
Department of Engineering Sciences  
26389 Wilhelmshaven, Germany  
nick.ruessmeier@jade-hs.de

Oliver Zielinski<sup>2,3</sup>

<sup>2</sup> German Research Center for Artificial Intelligence  
DFKI Laboratory Niedersachsen, Marine Perception  
26129 Oldenburg, Germany

<sup>3</sup> Carl von Ossietzky University of Oldenburg, Institute for Chemistry  
and Biology of the Marine Environment (ICBM)  
26382 Wilhelmshaven, Germany  
oliver.zielinski@dfki.de

**Abstract**—The natural dynamics of tidal currents continuously change the appearance of the Wadden Sea. Especially coastal regions and bays with shallow waters are strongly influenced by tidal dynamics. Meanwhile, in offshore study areas with harsh environmental conditions as well as dynamic ocean currents and water levels, continuous in-situ investigations of the prevailing current conditions requires a high effort. In-situ measurement technology is thereby maintenance-intensive and partly limited in time or space by limited accessibility or restricted by the measurement method. In hence, remote sensing techniques based on video image information, such as Large Scale Particle Image Velocimetry (LSPIV) for sensing, and computer vision algorithms for long-term investigation of the prevailing dynamic near-surface ocean flow conditions, have become highly relevant. However, in some environmental situations there may be not sufficient or significant natural textures evaluable in the visual camera images, or only insufficient contrast ratio under varying ambient illumination at the water observation site, to perform image based velocimetry. Thus, we consider with this study an extended approach of visual and infrared video data analysis by an automated LSPIV measurement technique under real offshore deployment conditions.

The treatise of this paper first introduces the reader to the subject area and technologies as well as the principles of the LSPIV measurement method. Followed by the depiction of the motivation for an extended approach to visual and infrared video data analysis by an automated LSPIV measurement method in real offshore applications. Subsequently, related research is discussed. Thereafter, the remote sensing setup and sensor-test-bed-system for offshore deployment on an observation platform is presented, therein we also addresses routines of necessary calibration procedures for camera sensors. We then depict details of our automated LSPIV measurement procedure. This is followed with an overview of the preceding validation procedures and LSPIV multispectral remote sensing results of long-term monitoring of horizontal flow dynamics over several days. Finally, we discuss uncertainties of the LSPIV velocity measurement method encountered in real applications and conclude with a brief outlook on further developments and applications.

**Keywords**—remote sensing, monitoring, offshore currents, North Sea; optical sensors, digital image processing, visual and infrared data stream, automated Large Scale Particle Image Velocimetry LSPIV, offshore currents, time series

## I. INTRODUCTION

The natural strong dynamics of tidal currents constantly change the appearance of the Wadden Sea. Especially bays with shallow waters, as they occur in coastal regions and tidal zones between islands, are strongly influenced by tidal dynamics [1]. Furthermore, the near-surface layer of seawater plays a crucial role for oceanographic-atmospheric processes [2, 3]. Optical sensor systems are therefore very relevant as a remote sensing tool for marine environmental research and operational applications [4]. High-quality data of in vertically resolved fluid dynamics are usually collected by in-situ measurements through acoustic profiling. However, this measurement technique is not applicable close to the air-water boundary layer due to strong backscatter interference. In addition, the maintenance effort for long-term operation of submerged measurement techniques will increase. Punctual measurement techniques, such as radar- or laser- Doppler flow sensors, on the other hand operate contactless, installed above the water surface. These techniques are often used for the continuous measurement of surface flow velocity at well accessible open flumes, such as rivers and canals.

Specifically, Large Scale Particle Image Velocimetry (LSPIV) provides another non-contact measurement technique via camera-based optical velocimetry that can be used to measure the flow at the surface of a water body. Thereby, the measuring technology is independent of constituents within the water body, which extends its range of application, and the measuring sensors are unaffected by the fluid conditions in the flow cross-section to be measured. In addition, the non-contact measuring technology reduces the risk to personnel and measuring equipment when applied during extreme flow conditions [5].

Contactless measurement of near-surface oceanographic flow conditions in a sufficient spatial and temporal context, on the other hand, is still a challenge with the outlined technical capabilities. Affected by harsh and changing environmental conditions, dynamic current velocities, changing water levels and current directions and waves, or simply by less accessibility, the maritime domain presents a set of challenging and new boundary conditions for the LSPIV measurement procedure, compared to inland areas. However, automated remote sensing

technologies based on optical video sensor data and computer vision algorithms are now available for long-term sensing of horizontal sea surface currents, which can be used to measure highly non-uniform flow conditions including recirculating currents, strong cross currents, etc., or very low flow velocities [6].

### *The LSPIV Measurement Method*

LSPIV stands for "Large Scale Particle Image Velocimetry" and determines 2-D vector fields of a near-surface flow in a relatively large spatial coverage area. LSPIV technology [7] is based on the analysis of optical remote sensing information in spatiotemporal dimensions. In simplified terms, moving patterns (tracers) are recorded in a time-sequenced imagery by an optical imaging sensor, such as a video camera. Subsequently, the displacement of the pattern along x and y coordinates of the image matrix is analyzed by a cross-correlation matrix of image-pair patterns with e.g. discrete Fourier transform. A segmentation of the entire image matrix into smaller interrogation regions generates velocity vectors over the entire measurement field. By assigning a real world distance of the camera viewing area to the camera pixels, as well as the time difference between two acquired images, the displacement of a pattern from pixels/image sequence is transferred to spatial coordinates per time unit, e.g. (m/s) [8]. Typically, current applications use at least four fixed known control points within an observed scene to associate real world distance coordinates to the camera viewing area. An automated LSPIV measurement procedure requires sequential pre-processing and quality-oriented post-processing steps through data filtering mechanisms for long-term observations. This procedure is relevant for all types of large-area image based velocity measurement, independent of the spectral wavelength of the camera used for image acquisition.

## II. MOTIVATION

The applicability and assurances of the performance of the LSPIV measurement method demands on adequate image acquisition and image analysis tools, especially for oceanographic field studies when using naturally occurring tracers and environmental interferences are probable expected. However, with respect to all known restrictions so far, the LSPIV measurement method is in some situations the only applicable and simultaneously cost-effective remote sensing measurement method, to investigate the prevailing velocity conditions of a sea surface with a high temporal and spatial resolution. When the LSPIV measurement method is used for long-term observation with images in the visible band (red-green-blue, RGB), this method relies on naturally occurring LSPIV tracers, e.g. floating foam or surface waves in the environment. In case of insufficient availability or density distribution of these tracers, as well as in case of insufficient ambient illumination conditions, the measurement method is not capable to analyze sufficient measurement data.

With passive IR remote sensing, information of a surface can be derived from the infrared emissivity, and when applied to water, from a layer of only a few micrometers thickness. The infrared emissivity of seawater derived for nadir observations is in the range of  $\epsilon = 0.96 - 0.99$  for wavelengths relevant to thermal remote sensing and can therefore be considered high [3].

Infrared cameras, which are sensitive in the 7.5 – 13  $\mu\text{m}$  band, are independent of ambient illumination and can provide video data even during night-time. Solar interference is thus less limiting for these infrared sensors compared to visual camera observations. Furthermore, the LSPIV measurement technique may benefit from an extension of IR emission signatures from naturally occurring sea surface tracers (seeding), such as temperature gradients, drifting particles or drifting surface films with characteristic emissivity, in real offshore applications. In this context, ongoing research orients towards extending image data acquisition in (multispectral) wavelength ranges, as well as advanced computer vision approaches for oceanographic investigations.

We examine therefore by this study an extended approach of visual (400 – 700 nm band) and infrared (7.5 – 13  $\mu\text{m}$  band) video data analysis with an automated LSPIV measurement method for real field applications. For the development, testing and validation of new optical measurement techniques and optical remote sensing methods, we employ for this purpose our universally applicable sensor-test-bed-system with integrated data streaming technology and wireless remote data transmission in self-sufficient operation on an observation platform at sea [6].

## III. STATE OF THE ART APPLICATIONS AND RELATED WORK IN INLAND/OFFSHORE WATER STUDIES

### *A. Inland studies with visual and infrared camera sensors*

Applications and capabilities of the LSPIV remote sensing measurement technique based on visual camera imagery demonstrates reliable results in various hydrographic laboratory- and field-based applications involving inland waters, e.g., studies at flood-bearing rivers and flood conditions, as well exchange processes in estuaries [8–10]. A summary of several case studies for river surface flow measurement and available LSPIV software tools, is presented in this context by Flora [11], the applied technology and performance of this technique was in there also be addressed. A photogrammetric approach with multiple visual cameras to measure the 3-D velocity of a free surface flow was pursued by Trieu and Bergström [12]. The capability of the camera systems and the particle tracking algorithm has been first investigated with a laboratory measurement, performed on an open flow channel and was then applied to a field measurement on an inland river. The field of view in the case spanned 11 m  $\times$  8.2 m and the observation height was 12 m. Further inland water studies examines the performance, automated applications, and uncertainties of the LSPIV method [9, 13, 14].

Studies on inland waters also investigating approaches by combining visual and thermal infrared cameras to observe river surface currents, turbulence metrics, and exchange processes. Thus, Puleo, McKenna, Holland and Calantoni described in their study, which was conducted on a small coastal plain in 2014, a comparison of measured mean in-situ velocities and an image evaluation of 5 minutes length each under daylight and darkness conditions. The maximum expected velocities were less than 1 m/s. In the setup, a stationary visual and infrared camera was installed at about 5.7 m height, lateral to the considered river section of about 15 m width and 20 m length [15]. A small apparent temperature contrast of about 1.6  $^{\circ}\text{C}$ ,

from a thin turbulently mixed layer of cooler water near the river surface, was used as the thermal tracer signal. The tracer signal in the visible band was foam on the water surface. Images were acquired by using a  $1024 \times 768$  pixel RGB camera and a  $640 \times 480$  pixel FLIR SC660 thermal imaging camera in the long wavelength radiation range of  $7.5 - 13 \mu\text{m}$ , with a temperature resolution of about  $0.05 \text{ }^\circ\text{C}$  and at  $3.75 \text{ Hz}$  intervals. The study shows several approaches for optical velocity measurement, on the one hand for an optical current meter time stacking method (OCM, one-dimensional) and on the other hand for a Particle Image Velocimetry method (two-dimensional).

#### B. Offshore studies with visual / infrared camera sensors

Utilizing a mobile deployment from catamaran at sea, Garbe, Schimpf and Jaehne describe thermographic techniques for investigating dynamic processes at the air-sea boundary layer of the ocean [16]. Among other aspects, their approach considers a surface renewal model and the analytical function of the temperature distribution of an IR image as well as computation of the 2-D optical flux (no LSPIV) and the total temperature derivation from an IR image sequence. In this study, an Amber Galileo MWIR camera with a moderate resolution of  $256 \times 256$  pixels, sensitive to a wavelength range of  $3 - 5 \mu\text{m}$ , features a Noise Equivalent Temperature Difference,  $\text{NETD} = 25 \text{ mK}$ . The camera was mounted on a small cantilever on top of a catamaran to capture thermographic image sequences with a  $50 \times 50 \text{ cm}^2$  grid. The results of this field experiment demonstrate the applicability in harsh oceanic environments and benefits of low-noise infrared cameras for visualizing thermal transport processes.

In conclusion, camera-based mobile flow measurement is a promising new field measurement technique. The prerequisite for a widespread use, shall envelop efficient and universal development of the evaluation algorithms through further research results and the compensation of changing environmental conditions to enhance the performance of this technique [5].

## IV. METHODS

### A. Study area & observation platform

The oceanographic survey by a multispectral LSPIV method was performed from an offshore station (TSS) in the southern North Sea (German Bight) from October 18<sup>th</sup> to October 24<sup>th</sup> 2016. The observation platform (Fig. 1) for hydrographic and marine environmental parameters, is located between the islands of Langeoog and Spiekeroog at position  $53^\circ 45.016' \text{ N}$ ,  $007^\circ 40.266' \text{ E}$ . Both islands belong to the offshore back tidal flats of the East Frisian Islands with shallow water depths up to 20 m and form a natural flow channel (gat). The main water flow is topography guided and follows a westerly ( $\sim 284^\circ$ ) to easterly ( $\sim 104^\circ$ ) course between the islands at the measurement position for rising water conditions and a correspondingly opposite course while falling water conditions. The mean sea level (MSL) ranges 13 m at the observation platform. Strong semi-diurnal tidal cycles with a tidal amplitude of about 2.7 m, as well as high current velocities up to 2 m/s characterize the prevailing measurement conditions there [17, 18]. Comprehensive reference measurement data for meteorological, hydrographic and marine environmental parameters are available from this observation station. For example, tidal height measurement (calibrated ultrasonic sensor, LOG aLevel, General Acoustic, Germany), or wind conditions 12 m above mean sea level (METEROLOGY, Lambrecht, Germany).

### B. Remote sensing setup

Remote sensing for the LSPIV procedure was performed with two cameras in combination of a visual camera (acA2040-gc, Basler) and an infrared camera, type PI450 (Optris GmbH, Germany) based on a microbolometer focal plane array (FPA, uncooled), emission factor  $\epsilon = 0.96$ . The latter provides in addition to the visual camera, a video data stream in the infrared spectral range, with corresponding information of the sea surface temperature in the test field. For a better overview, the details of the camera systems used are summarized in Table 1. The selection of the camera systems considers beneath the

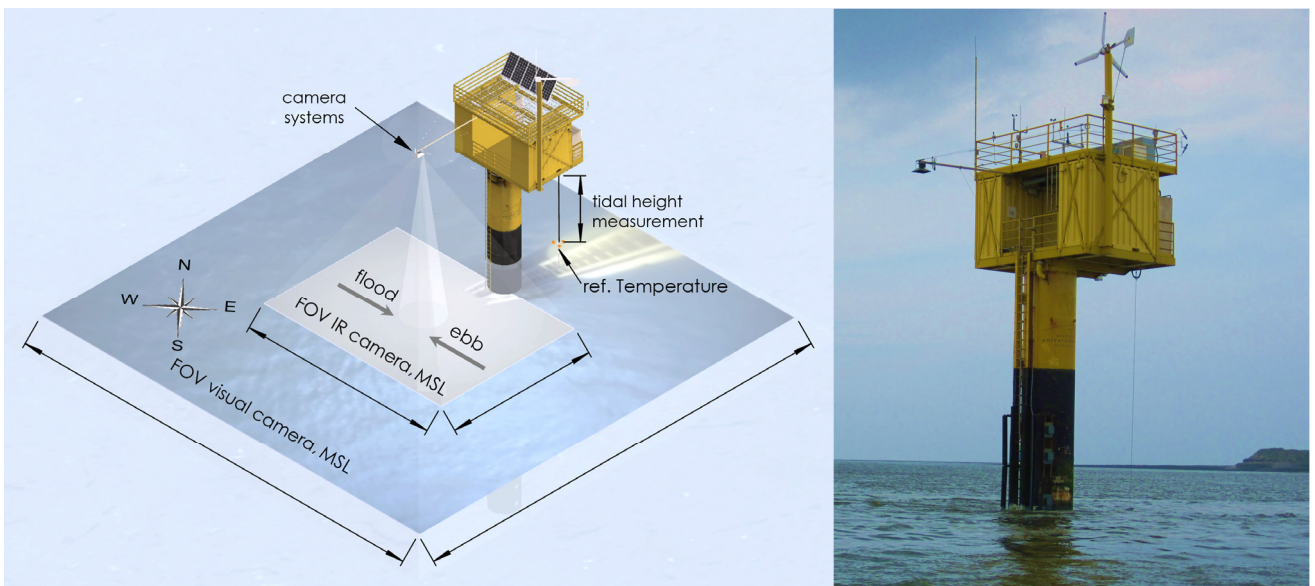


Fig. 1. Left: Schematic drawing of the observation platform showing the prevailing tidal flow directions and field of view from the different camera sensors as well as reference measurement systems. Right: Photo of the system setup in the real offshore environment near the island Spiekeroog.

optical characteristics, available data stream interfaces (USB/GigE Vision), documentation, SDK (Software Development Kit), hardware drivers, available interchangeable lenses and the price-performance ratio. On the observation platform, the cameras were deployed closely side-by-side with a stabilized cantilever, 9.9 m above mean sea level (MSL) in nadir view to the sea surface. The overlapping field of view (FOV) of both camera systems at mean sea level (MSL) is illustrated in Fig. 1, top left.

### C. Characterization and calibration of the camera systems

A characterization of the infrared camera and IR optics forms, analogous to the visual camera-lens combination, a basis for the targeted use in various applications. In addition to the optical resolution of an infrared camera, the thermal sensitivity (Noise Equivalent Temperature Difference, NETD), the thermal resolution and system stability is also important for temperature measurement in real study conditions. The intrinsic camera parameters, including radial symmetric distortion, were therefore measured in the laboratory for both camera systems prior to field use, and these will be then corrected during the subsequent LSPIV analysis. In addition, the radiometric distortion with NUC (non-uniformity-correction) and the thermal sensitivity as well as long-term stability for the temperature range to be measured were examined for the IR camera.

Since a conventional calibration grid for measuring the intrinsic parameters and radial symmetric distortion for visual cameras does not provide evaluable IR signatures, a spatial test grid with coded targets was used for the IR camera [19]. For all measurements very small aberrations, mostly below 20  $\mu\text{m}$  (detector pixel size 25  $\mu\text{m}$ ) were observed, i.e. below 1 pixel.

When investigating the radiometric distortion under laboratory conditions, the absolute measured temperature in the center of the FPA sensor matrix deviates by 0.05 K from an external reference temperature (20.05 C) and is thus still sufficient for the intended purposes of maritime environmental

monitoring. Higher deviations of up to 0.7 K from the absolute reference temperature occur at the image edges and can be attributed to projection-dependent radiometric distortions of the optics of an IR camera, as also published in other studies [20]. The effect will be accounted by correction factors in the image data pre-processing step for the LSPIV method. Under ideal circumstances, internal NUC camera parameters should ensure equal temperature values over the entire microbolometer matrix [21].

Due to the uncooled focal plane array of the IR camera, it features an internal housing- and FPA-heating for temperature stabilization (above the external temperature), as well as an internal FPA temperature calibration by using of a mechanical shutter (flag), otherwise the measured temperature values will drift over time. During the long-term field operation, an internal automatic calibration of the camera with 12 s flag interval was carried out and a stability of the temperature measurement of  $\pm 0.25$  K was guaranteed. For the temperature stabilization in the field, the camera has to warm up for about 40 minutes, measurement activities should thus begin only after an adequate stabilization time when deploying. Similar warm-up times were also observed in other studies [22]. The temperature stability is mainly limited by drift of the microbolometer FPA [23], and for our camera system still sufficient for the applications in the field of marine environmental observation.

### D. Sensor-test-bed-system and data stream management

For the development, testing and validation of new optical sensors as well as measurement methods for optical remote sensing, a sensor-test-bed-system with integrated sensor data stream management has been developed and already applied in different maritime study areas [24, 25]. The sensor-test-bed-system provides multiple functionalities for the general management of different sensors as well as the continuous recording of video data with relevant corresponding sensor metadata, such as specific camera model parameters and the UNIX millisecond time stamp for each video frame.

For a universal applicability, the data stream management system manages over 300 different codecs for processing a wide variety of video sources by an FFmpeg as well as OpenCV multimedia library. However, a commonly standardized radiometric video data stream format has not yet been established for microbolometer IR cameras. For a storage efficient long-term data acquisition of the IR- video data stream (radiometric measurement values, 16-bit 1-channel temperature image), the sensor data stream management system processes the IR camera data stream to a 32-bit RGBA image with standardized FFV1 video codec. Thus, the storage of the radiometric readings is done as a "non-compliant" 32-bit pixel .avi format and requires a separate virtual video decoder for an out-of-system reuse, e.g. in Matlab. The continuously data stream acquisition of the two cameras was performed by means of the sensor-test-bed-system, and for the visual camera with a fixed exposure time. Remote access to the offshore-stationed sensor-test-bed-system was achieved via an LTE connection. For the long-term operation application presented herein, this constitutes a substantial reduction in effort, time saving and quality control options, since no on-site presence in the study environment is required, shown in Fig. 2.

TABLE I. OVERVIEW OF CAMERA SENSOR SPECIFICATIONS

Specification	Video camera system		
	Unit	Visual	Infrared
Type		acA2040-gc, RGB, Basler	PI 450, Optris microbolometer
Detector (Pixel Size)	$\mu\text{m}$	CMOS (5.5 $\times$ 5.5)	FPA, uncooled (25 $\times$ 25)
Optical resolution	Pixel	2048 $\times$ 2048	382 $\times$ 288
Type Lens		LM6HC, Kowa Optimed	Optris
Field of view	deg	97 $\times$ 97	62 $\times$ 49
Focal length	mm	6	8
Frame rate (record)	Hz	20	27
Radiometric resolution	bit	8	16
Thermal sensitivity (NETD)	mK	–	40
System accuracy (at T <sub>Amb</sub> = 23 $\pm$ 5 $^{\circ}\text{C}$ )	%	–	$\pm 2$
Spectral range	$\mu\text{m}$	4 – 7	7.5 – 13

## V. AUTOMATED LSPIV MEASUREMENT TECHNIQUE

The automated LSPIV remote sensing is based on our previous software development and the details of the individual process and video data analysis steps for data input, image data pre-processing, calibration as well as quality oriented post-processing steps, have been comprehensively presented [6]. For this study, we use the identical automated LSPIV measurement procedure for continuous long-term observation of the horizontal flow velocities and flow directions in the maritime environment. All computations were realized in Matlab Release 2019b (MathWorks, Inc.) and consider extensive processing steps as implemented in complementary LSPIV analysis tools for inland studies such as Fudaa or RIVeR [26]. The LSPIV system for long-term monitoring based on adaptive and extended functions of PIVlab ver.1.41 [27]. Through the extension, e.g. any video data or video data stream can be directly transferred to the LSPIV analysis and be automatically processed and evaluated for long-term observations. In addition, further statistical parameters and averaging temperature matrixes are supplied.

When setting up an LSPIV measurement system as well as data analysis, certain aspects should be considered to achieve reliable results with minimal uncertainties. System-based systematic error sources should be mentioned in this context, starting from the camera setup, raw data acquisition and data pre-processing. As well as random errors such as those caused by changing environmental conditions may occur, the details and relevance of the latter are therefore discussed in Chapter VI. Regarding the latter, we introduce in the following correction parameters and georectification for the LSPIV method for this study and the prevailing environmental conditions. Afterwards, an overview of the LSPIV pre-processing, image analysis, and post-processing methods and parameters are presented.

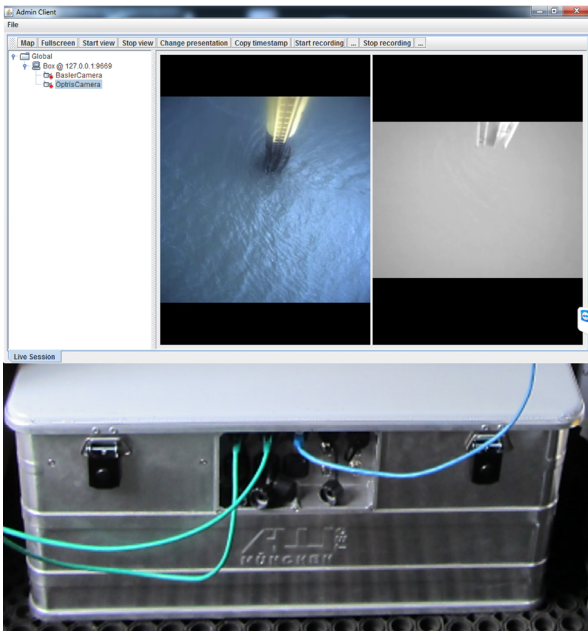


Fig. 2. Top: Visualization of the (visual/infrared) video camera images from the sensor-test-bed-system from the observation platform with a view on the sea surface. Bottom: Sensor-test-bed-system in offshore use with remote data access.

### A. Correction parameters and georectification

Due to the prevailing tidal amplitude at the study area, the distance ( $\Delta h$ ) between the seawater surface and the fixed cameras at the observation station changes alternately, and thus also the specific camera field of view (FOV). For a FOV current velocity correction in the LSPIV calculation procedure, the tidal amplitude (tidal height measurement) was therefore measured via a calibrated ultrasonic sensor from the observation platform, shown in Fig. 3, top.

As explained formerly, image based quantitative velocity measurement requires georectification of image plane coordinates ( $U, V$ ) into real coordinates grid ( $x, y, z$ ). Offshore observations often miss fixed or well-known reference or location control points in the image. Therefore, a georectification as commonly used in other inland field studies [28], to assign from a camera field of view to geospatial pixel coordinates, can only be applied with significant effort at offshore study areas and is not effectively feasible.

We use therefore an alternative approach through a camera orthorectification coefficient which calculates the pixel distance coordinates for the known camera viewing angle, under consideration of the distance to the surface and camera and lens parameters (FOV) [6]. The correction factor is then applied to the velocity measurement data by the LSPIV post-processing procedure. In this study case, we obtain an alternating FOV of about  $200 - 370 \text{ m}^2$  for the visual camera and about  $45 - 75 \text{ m}^2$  for the infrared camera, presented in Fig. 3 bottom. Concomitantly, in this field application, we obtain a true pixel resolution of  $7 - 9 \text{ mm/pixel}$  with the visual camera and  $20 - 27 \text{ mm/pixel}$  for the infrared camera.

### B. Video image data pre-processing

Pre-processing can be used to differentiate suitable tracer signatures in the image from the surrounding environment, so the RAW image (raw data format) is optimally prepared for further LSPIV analysis. This was carried out by the routine PIVlab functions for Adaptive Histogram Equalization

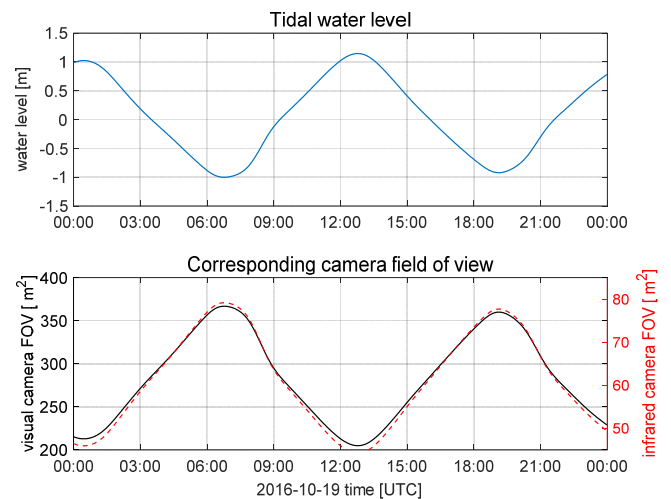


Fig. 3. Top: Tidal water level (MSL) derived from TSS measurements with ultrasonic sensor showing semi-diurnal tidal cycles in the range of about 2.2 m. Bottom: Calculated corresponding camera FOV, visible camera (left axes) and infrared camera (right axis), representation for one day

(CLAHE) in small image areas, intensity high-pass filter and intensity adjustment. The parameters for the different image processing filters as well as the frequency-dependent histogram filters need to be chosen in according to the raw image data format. An optimal pre-processing process would subsequently pass only a black and white image (black as background and white as tracer) to the LSPIV peak finding image evaluation.

For this study and the prevailing environmental conditions, appropriate pre-processing settings were determined for the visual camera images (RGB color image) with a CLAHE window size of 128 pixels, a high-pass filter size of 20, and active intensity adjustment. For the pre-processing of the RAW infrared camera images (temperature matrix), further functions were implemented in the automated LSPIV pre-processing process to perform an Adaptive Temperature Equalization, intensity high-pass filter and intensity adjustment, based on the mean of the distribution temperature matrix. In the subsequent step, the temperature matrix with 16-bit resolution is mapped to a grayscale table and converted to an 8-bit grayscale image. An example in Fig. 4 left and center, reveal the comparison between a raw temperature matrix grayscale image from the infrared camera (unprocessed) and the result after image pre-processing with perfect quality for a LSPIV analysis.

#### C. Automated LSPIV-Settings with Discrete Fourier Transformation (DFT)

By using the adapted automated LSPIV measurement procedure, thus a continuous velocity time series of vector fields of a near-surface flow is provided. However, the main interest of this work resides in a long term evaluation of the prevailing current velocity and direction in an area that will not be disturbed by the construction of the observation station. A region of interest (ROI) was therefore applied to the image and subsequently analyzed to obtain surface flow conditions for long-term observation which are as far as possible undisturbed by the measuring pile. The image evaluation calculates the (displacement) vector of signatures between two image-pairs of the ROI. For this purpose, frame A1 and B1 are divided into a uniform grid with small query regions  $A_{(i,j)}$ ,  $B_{(i,j)}$ . The cross-correlation matrix  $C_{(m,n)}$  will then be computed using discrete Fourier transform (DFT) for each of these interrogation regions with multiple passes for partial overlaps from  $B_{(i,j)}$  to  $A_{(i,j)}$  via PIVlab functions [27]. As a result, 2-D vector fields and the

standard deviation for each of the interrogation windows are computed, shown in Fig. 4 on the right. The calculation parameters can be freely set as needed for the particular camera viewing area, the expected flow velocity variables and the dynamic range to be covered.

For the visual camera, we chose an image-pair sampling rate of 1 Hz and  $\Delta t = 50$  ms time steps between two ensembles of the images, the initial query window size was 128 pixels with a step size of 64 pixels and one pass. The infrared camera image-pair sampling rate was also 1 Hz with  $\Delta t = 135$  ms time steps between two corresponding images. Due to the lower image pixel-resolution the initial interrogation window size was chosen by 64 pixels, with two interrogation steps of step size 32 and second window size of 16.

#### D. Post-processing parameter and LSPIV-Output

Since the LSPIV results of the calculated velocity vectors rely on statistical evaluation methods, they may be erroneous and usually need to be post-processed to obtain reliable results. Therefore, comprehensive regions such as paths or areas in the study area should be subdivided according to the investigation objectives for the long-term analysis of the prevailing flow velocity and flow direction conditions. With the post-processing, unrealistic velocity vectors in the ROI are classified in terms of their standard deviation of direction and magnitude in relation to the normal distribution in the vector field, whereas these results become then filtered out. The post-processing filtering steps must be carefully parameterized to distinguish between the real velocity conditions and random errors caused by environmental interferences. Post-processing also applies the tidal amplitude-dependent orthorectification coefficient with the true pixel resolution and thereby the real velocity is calculated. Furthermore, an assignment of the north direction (azimuth) to the measured camera orientation is applied for a more accurate positional orientation of the flow direction.

The result of the automated LSPIV analysis contains a time series of the corrected flow velocity matrix, its mean value from the considered ROI of an image scene and in addition the respective standard deviation and median temperature results are included in the measurement.



Fig. 4. Left and Center: Shows the comparison between a temperature matrix as a grayscale image from the infrared camera (unprocessed) and the result after image pre-processing with perfect quality. It can be seen that the tracer points become highlighted and segmented, but minimal noise remains in the background, which can lead to higher standard deviations in the LSPIV analysis. Right: Another IR scene during darkness around midnight with region of interest in front of the observation platform, for a long-term observation of undisturbed sea surface current conditions, with superimposed LSPIV vector field

## VI. VALIDATION, RESULTS AND DISCUSSION

### A. Validation

During a continuous observation period of 11 hours, we used the LSPIV method in a previous offshore study in the German Bight in the Wadden Sea to collect a valid database of the near-surface current velocity as well as the normal fluctuations of a tidal current direction within a daily cycle [6]. Thus, it became

possible to consider a complementary approach to fuse horizontal flow measurement data and vertically resolved in-situ measurements from an Acoustic Doppler Current Profiler (ADCP). For validation in the previous study, the identical system setup with the visual camera was aligned in nadir view 9.9 m above mean sea level and video images with signatures of natural tracers in the spectral range of 400 – 700 nm were automatically analyzed using the LSPIV method. With the

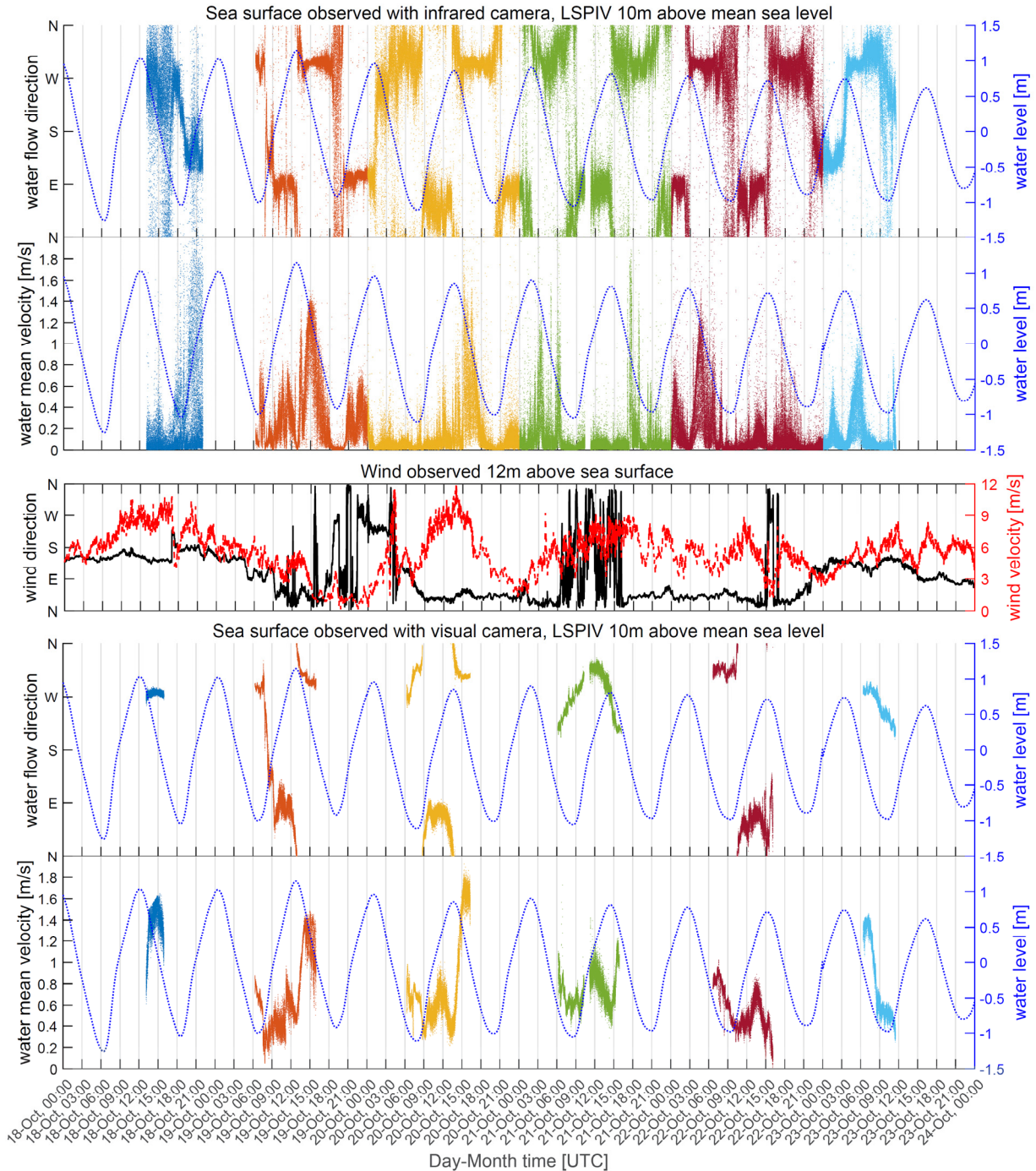


Fig. 5. Offshore collected LSPIV time series for magnitude current velocity and current direction, obtained from the region of interest. Results of the infrared camera in the upper diagram, visual camera in the lower diagram, the respective tide amplitude is shown in the background as dashed line. The respective prevailing wind conditions are presented in the middle diagram.

constraint of appropriate illumination conditions, the correlation coefficient of flow velocity from LSPIV and comprehensive in-situ reference measurements within a tidal cycle was  $r^2 = 0.82$  in this case, and tidal dynamics could be captured with a minimum response of 0.15 m/s. With negligible wind effects, the correlation coefficient of the flow directions at the sea surface was  $r^2 = 0.83$ . This study further demonstrated relevant sources of uncertainty for measurements with a visual video camera. The measurement inaccuracy of the current velocity can be attributed to insufficient tracer availability and illumination or unfavourable illumination conditions, such as variations in illumination intensity or sun glint at the water surface. The latter occurred specifically at zenith angles  $\theta_s$  ( $17^\circ \leq \varphi \leq 17^\circ$ ), i.e. around noon and solar radiation maximum.

### B. Results

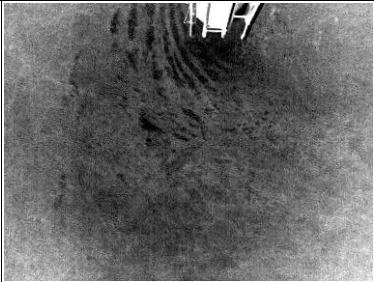
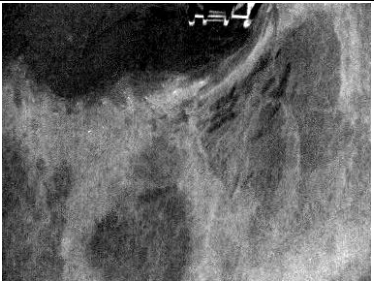
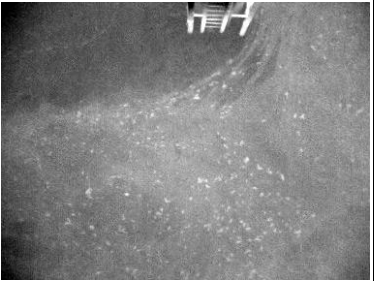
With the LSPIV time series and the multispectral camera setup from the offshore observatory, we provide an insight into near-surface oceanographic flow conditions during the period from October 18<sup>th</sup> to October 24<sup>th</sup> 2016. Fig. 5 shows comparative LSPIV results for the average mean flow velocity and flow direction of the ROI from the two camera systems. The LSPIV data based on the infrared camera at the top and the visual camera at the bottom. Complementary, the respective tidal amplitude (base MSL) is superimposed in the figures. Prevailing wind speed and wind direction are shown in the middle of of Fig.5. For better visualization, each LSPIV dataset of a day has been color separated (due to maintenance, data in the period 18<sup>th</sup> 17:00 UTC to 19<sup>th</sup> 06:00 UTC is not included). The six-day observation period covers daytime and night-time observations with some moderate and some high and turbulent wind conditions (evident from rapid wind direction changes), as well as several semi-diurnal tidal cycles with high water and low water, slack water and omnidirectional flow conditions (evident from flow direction reversals from west to east and vice versa). For LSPIV remote sensing with the visual camera sensor, only data during sufficient natural illumination is obtainable, no data are available at dusk or at night. In contrast, coherent information is available from the thermal camera datasets, regardless of the time of day.

For the surface flow velocity measurement, a strong influence of the prevailing wind effects on the water surface is evident. This affects the remote sensed data information from both camera systems, for example in the period from 20<sup>th</sup> 00:00 UTC to 21<sup>th</sup> 09:00 UTC with high wind speeds, at this period no sufficient LSPIV velocities could be calculated. The wind effect leads to high inhomogeneous, distributed and scattered velocity components in the flow vector matrices and consequently data getting filtered out by the LSPIV post-processing analysis due to the high standard deviation. High temporal resolution LSPIV analyses furthermore permit the observation of wind shear components acting on the surface water body [29]. For the thermal camera data, there are also deviations in the context of different image quality levels which we would like to discuss in the following, for example in the period 21<sup>th</sup> 08:00 UTC to 17:00 UTC. The analysis data of the time series for the prevailing flow direction can be derived with both, visual and infrared camera systems, and the dataset is fully available via the thermal camera system.

### C. Discussion

Field-based LSPIV generally relies on the texture of naturally present tracer textures in the image, such as surface foam or other flotsam and surface waves. These are typically present in offshore areas and are detectable by visual image analysis. For LSPIV based on RGB camera sensors, the natural water surface of interest requires sufficient illumination by ambient illumination in the image scene and its performance is optimal under overcast conditions. Direct sunlight leads to errors in the LSPIV image evaluation process due to scattering and reflections on the water surface. The consequences are uneven as well as scattered velocity vectors and therefore incomplete measurement data. Within an analyzed flow time series, the described effects have an impact during the quality-oriented data post-processing in the form of a higher standard deviation in the calculated LSPIV measurement results. In summary, LSPIV with visual remote sensing can provide sufficient data from significant natural textures in a wide variety of environmental situations, but is temporally limited due to insufficient natural illumination at the observation site to perform an image based velocity measurement.

TABLE II. QUALITY LEVELS OF MEASUREMENT DATA

Scenery characteristic	Example of different quality levels of measurement data for an LSPIV image evaluation process.		
	a) Poor measurement scene	b) Good measurement scene	c) Perfect measurement scene
Example IR-Image			
Tracer distribution	noisy image, less tracer	contiguous extensive, recognizable	numerous, separated and detached
Tracer contrast	no discrete particle or pattern recognizable	less significant points	significant tracer points
Temperature distribution	homogeneous temperature distribution	clear inhomogeneous temperature distribution recognizable	inhomogeneous temperature distribution recognizable



Using thermal camera systems, tracers of different temperature or IR emission gradients from drifting particles or drifting surface layers are also available during darkness. Especially during long-term investigations, a wide variety of environmental situations and diverse formations of image tracer signatures on the water surface occur and must be taken into account during LSPIV image pre-processing. Some examples of different sea surface infrared camera image quality levels are therefore provided in Table 2. There are environmental situations where tracers with only a low image contrast, respectively discrete temperature distribution are present, shown in Table 2a) or only large scale and coherent tracer distributions occur, shown in Table 2b). An excellent image scene for the LSPIV measurement method is shown in column c) of Table 2. The temperature scaling in all scenes is about 11.8 °C to 13.2 °C and the difference temperature of the signatures is thus about 1.5 °C.

The advantage in the new application scope with the deployment in offshore study areas is opposed by an increased effort to collect reference and correction data, such as tidal amplitude. The influence of wind, for example, can greatly affect the measurement of surface velocity, thus parallel gathering of wind direction and wind speed is recommended. Due to the variability of the environment and remote sensing scenes, qualitative limitations of the spatial resolution in the form of random errors of an LSPIV analysis are thus to be expected. The latter then present themselves with a high standard deviation or erroneous measured values, as also shown in other inland field studies [14]. In such cases, a very large interrogation window and step size (LSPIV) can be used to evaluate average values of a displacement vector on basis of the cross-correlation matrix with the Discrete Fourier Transform (DFT) over the entire image scene, whereby the spatial resolution of the vector fields of a scene is reduced. On the other hand, it would be possible to evaluate image-pairs using Direct Cross Correlation (DCC), although this method is comparatively more ineffective in terms of the computation time required, varying in accordance to the image pixel resolution. In this relation, Thielke and Sonntag present a review of the performance and robustness for the analysis of different texture types with corresponding bias and RMS errors of the PIVlab tool. This lists erroneous correlation estimates of up to 70% for noisy images without tracers [30]. Which measurement and evaluation strategy and combination of camera sensors and computer vision algorithms for LSPIV evaluation in a field application is most suitable must be determined individually depending on the particular observing objective.

In summary, we can conclude that customized image data pre-processing algorithms for a wide range of multispectral camera systems, as well as the extensions for efficient video data stream processing for continuous acquisition of temporally high-resolution flow events, can be used to realize long-term investigations over several days with the sensor-test-field-system. Naturally occurring tracers in the marine environment can be detected with limitations both during the day with the visual camera and with a microbolometer infrared camera (7.5 – 13 µm band) independent of natural illumination and can be applied for LSPIV remote sensing of near-surface flow conditions. Up to now, our approaches to LSPIV-remote sensing

with visual camera technology were limited in temporal resolution.

A combination of visual and infrared camera technology thus increases the possibility of recording usable information on the state of the environment even in difficult environmental situations. The image pixel-resolution as well as temperature sensitivity of the deployed camera systems was sufficient for the observed scene and did not pose any limitations for a long-term LSPIV observation. Even strongly non uniform flow conditions with backflows, strong crossflows etc. can be measured and visualized. In the environment under observation, it is important that natural tracers are available with sufficient quality to minimize errors in automated image analysis. This proved to be a limiting factor in our offshore application study.

With this offshore application study, long-term spatio-temporally resolved ocean current conditions could be made accessible for marine science and other applications by LSPIV remote sensing, and useful information for further expansion stages and algorithms of the sensor system were gathered. Therefore, we already address the required approaches for multispectral data fusion of different sensors in ongoing studies. In the future, also mobile LSPIV applications on board of vessels can provide new insights for the research and development of remote sensing, with promising and useful applications for the assessment of the state of the seas and further exploration of oceanic environments and inland waterways.

#### DATA AVAILABILITY

The data and LSPIV analysis tool presented in this paper are available upon request from the corresponding presenting author. Real-time data from the TSS Spiekeroog are available at <https://uol.de/icbm/forschungsplattformen-schiffe/messstation/echtzeitdaten>.

#### ACKNOWLEDGMENT

The authors would like to thank the team of the Time Series Station Spiekeroog for the support with technical assistance in all our experimental work. We would also like to express our gratitude to Nico Jordan for assistance of verifying measurement data. DFKI acknowledges financial support by the MWK through “Niedersachsen Vorab” (ZN3480).

#### REFERENCES

- [1] L. Holinde, T. H. Badewien, J. A. Freund, E. V. Stanev, and O. Zielinski, “Processing of water level derived from water pressure data at the Time Series Station Spiekeroog,” *Earth Syst. Sci. Data*, vol. 7, no. 2, pp. 289–297, 2015, doi: 10.5194/essd-7-289-2015.
- [2] O. Wurl, W. Ekau, W. M. Landing, and C. J. Zappa, “Sea surface microlayer in a changing ocean – A perspective,” *Elementa: Science of the Anthropocene*, vol. 5, 2017, doi: 10.1525/elementa.228.
- [3] A. Soloviev and R. Lukas, *The Near-Surface Layer of the Ocean: Structure, Dynamics and Applications*, 2nd ed. Dordrecht, s.l.: Springer Netherlands, 2014.
- [4] C. Moore et al., “Optical tools for ocean monitoring and research,” *Ocean Sci.*, vol. 5, no. 4, pp. 661–684, 2009, doi: 10.5194/os-5-661-2009.
- [5] G. Morgenschweis, *Hydrometry: Theory and practice of flow measurement in open channels; Hydrometrie: Theorie und Praxis der Durchflussmessung in offenen Gerinnen*, 2nd ed. Berlin: Springer Vieweg, 2018.

- [6] N. Ruessmeier, A. Hahn, and O. Zielinski, "Ocean surface water currents by large-scale particle image velocimetry technique," in OCEANS 2017 - Aberdeen: 19-22 June 2017, Aberdeen, United Kingdom, 2017, pp. 1–10.
- [7] I. Fujita, M. Muste, and A. Kruger, "Large-scale particle image velocimetry for flow analysis in hydraulic engineering applications," *Journal of Hydraulic Research*, vol. 36, no. 3, pp. 397–414, 1998, doi: 10.1080/00221689809498626.
- [8] A. Schroeder and C. E. Willert, *Particle Image Velocimetry: New Developments and Recent Applications*. Berlin, Heidelberg: Springer-Verlag Berlin/Heidelberg, 2008.
- [9] J. Le Coz, A. Hauet, G. Pierrefeu, G. Dramais, and B. Camenen, "Performance of image-based velocimetry (LSPIV) applied to flash-flood discharge measurements in Mediterranean rivers," *Journal of Hydrology*, vol. 394, 1-2, pp. 42–52, 2010, doi: 10.1016/j.jhydrol.2010.05.049.
- [10] A. J. Bechle and C. H. Wu, "An entropy-based surface velocity method for estuarine discharge measurement," *Water Resour. Res.*, vol. 50, no. 7, pp. 6106–6128, 2014, doi: 10.1002/2014WR015353.
- [11] K. Flora, *Flood Flow Estimation using Large Scale Particle Image Velocimetry (LSPIV)*. [Online]. Available: <https://dot.ca.gov/-/media/dot-media/programs/research-innovation-system-information/documents/preliminary-investigations/flood-flow-pi-0208171-a11y.pdf> (accessed: Jul. 12 2021).
- [12] H. Trieu, P. Bergström, M. Sjödhall, J. G. I. Hellström, P. Andreasson, and H. Lycksam, "Photogrammetry for Free Surface Flow Velocity Measurement: From Laboratory to Field Measurements," *Water*, vol. 13, no. 12, p. 1675, 2021, doi: 10.3390/w13121675.
- [13] Q. Ran, W. Li, Q. Liao, H. Tang, and M. Wang, "Application of an automated LSPIV system in a mountainous stream for continuous flood flow measurements," *Hydrol. Process.*, vol. 30, no. 17, pp. 3014–3029, 2016, doi: 10.1002/hyp.10836.
- [14] Y. Kim, *Uncertainty analysis for non-intrusive measurement of river discharge using image velocimetry: The University of Iowa*, 2006.
- [15] J. A. Puleo, T. E. McKenna, K. T. Holland, and J. Calantoni, "Quantifying riverine surface currents from time sequences of thermal infrared imagery," *Water Resour. Res.*, vol. 48, no. 1, 2012, doi: 10.1029/2011WR010770.
- [16] C. Garbe, U. Schimpf, and B. Jaehne, "Measuring important parameters for air-sea heat exchange," in *Thermosense XXIV*, Orlando, FL, 2002, pp. 171–182.
- [17] B. Baschek et al., "The Coastal Observing System for Northern and Arctic Seas (COSYNA)," *Ocean Sci.*, vol. 13, no. 3, pp. 379–410, 2017, doi: 10.5194/os-13-379-2017.
- [18] R. Reuter, T. H. Badewien, A. Bartholomä, A. Braun, A. Lübben, and J. Rullkötter, "A hydrographic time series station in the Wadden Sea (southern North Sea)," (in En;en), *Ocean Dynamics*, vol. 59, no. 2, pp. 195–211, 2009, doi: 10.1007/s10236-009-0196-3.
- [19] T. Luhmann, J. Piechel, and T. Roelfes, "Geometric calibration of thermographic cameras," in *Thermal infrared remote sensing : sensors, methods, applications*, Dordrecht [u.a.]: Springer, 2013, pp. 27–42.
- [20] A. Tempelhahn, H. Budzier, V. Krause, and G. Gerlach, "Shutter-less calibration of uncooled infrared cameras," *J. Sens. Sens. Syst.*, vol. 5, no. 1, pp. 9–16, 2016, doi: 10.5194/jsss-5-9-2016.
- [21] T. Hoelter and B. Meyer, "The challenges of using an uncooled microbolometer array in a thermographic application," RAYTHEON CO GOLETA CA, 1998. [Online]. Available: <https://apps.dtic.mil/sti/pdfs/ADA399432.pdf> (accessed: Jul. 12 2021).
- [22] Krzysztof Kusnierek and Audun Korsath, "Challenges in using an analog uncooled microbolometer thermal camera to measure crop temperature," *International Journal of Agricultural and Biological Engineering*, vol. 7, no. 4, pp. 60–74, 2014, doi: 10.3965/j.ijabe.20140704.007.
- [23] P. W. Nugent and J. A. Shaw, "Calibration of uncooled LWIR microbolometer imagers to enable long-term field deployment," in *Infrared Imaging Systems: Design, Analysis, Modeling, and Testing XXV*, Baltimore, Maryland, USA, 2014, 90710V.
- [24] M. Günther, F. Kammler, O. Ferdinand, J. Hertzberg, O. Thomas, and O. Zielinski, "Automatic recognition of individual Objects with the Dynamic Anchoring Agent," "Automatische Wiedererkennung von individuellen Objekten mit dem Dynamic Anchoring Agent," *HMD*, vol. 57, no. 6, pp. 1173–1186, 2020, doi: 10.1365/s40702-020-00675-y.
- [25] N. Rüssmeier, A. Hahn, D. Nicklas, and O. Zielinski, "A research port test bed based on distributed optical sensors and sensor fusion framework for ad hoc situational awareness," *J. Sens. Sens. Syst.*, vol. 6, no. 1, pp. 37–52, 2017, doi: 10.5194/jsss-6-37-2017.
- [26] A. Patalano and C. Garcia, "RIVeR—Towards affordable, practical and user-friendly toolbox for Large Scale PIV and PTV techniques," in *River flow 2016: Proceedings of the International Conference on Fluvial Hydraulics (River Flow 2016)*, St. Louis, USA, 11-14 July 2016, Taylor & Francis Group, 6000 Broken Sound Parkway NW, Suite 300, Boca Raton, FL 33487-2742, 2016.
- [27] W. Thielicke and E. J. Stamhuis, "PIVlab – Towards User-friendly, Affordable and Accurate Digital Particle Image Velocimetry in MATLAB," *Journal of Open Research Software*, vol. 2, no. 1, 2014, doi: 10.5334/jors.bl.
- [28] K. Holland, R. A. Holman, T. C. Lippmann, J. Stanley, and N. Plant, "Practical use of video imagery in nearshore oceanographic field studies," *IEEE J. Oceanic Eng.*, vol. 22, no. 1, pp. 81–92, 1997, doi: 10.1109/48.557542.
- [29] A. A. Grachev, C. W. Fairall, J. E. Hare, J. B. Edson, and S. D. Miller, "Wind Stress Vector over Ocean Waves," *Journal of Physical Oceanography*, vol. 33, no. 11, pp. 2408–2429, 2003, doi: 10.1175/1520-0485(2003)033<2408:WSVOOW>2.0.CO;2.
- [30] W. Thielicke and R. Sonntag, "Particle Image Velocimetry for MATLAB: Accuracy and enhanced algorithms in PIVlab," *Journal of Open Research Software*, vol. 9, 2021, doi: 10.5334/jors.334.